Iron loss comparison of standard SiFe and nanocrystalline materials for power transformers in a dual active bridge converter

Tobias Kauder and Kay Hameyer
Institute of Electrical machines (IEM), RWTH Aachen University
Schinkelstr. 4
Aachen, Germany
Tel.: +49 / (241) – 80 97667
Fax: +49 / (241) – 80 92270
E-Mail: Tobias.Kauder@iem.rwth-aachen.de
URL: http://www.iem.rwth-aachen.de

Acknowledgements

This work is supported by the cooperative project FEN (Flexible Electric Networks) which is funded by the German Federal Ministry of Education and Research under Grant 03SF0489.

Keywords

«High frequency power converter», «Magnetic measurement», «Material modelling», «Medium frequency transformer»

Abstract

This paper presents an analysis of different structured ferromagnetic materials for medium frequency applications. Metrological characteristics are performed at standardized instruments made by Brockhaus, i.e., Epstein frames and ring coil testing module. The final application is a transformer core used in a galvanically isolated phase-shifted dc-dc converter. The efficiency of a dual-active-bridge (DAB3) DC-DC converter is influenced, among others, by the iron losses of the medium frequency transformer. The iron losses of grain-oriented SiFe, non-oriented SiFe and nanocrystalline materials are measured at medium frequencies up to several kilohertz under sinusoidal excitation. The IEM-5-Parameter iron loss formula, which is based on semi-physical parameters, is used to evaluate the material characteristics. In addition, the excitation signal is adapted to the DAB3 application. The signal is examined by using a fast Fourier transform. The semi-physical iron loss separation model is adapted to consider the occurring harmonics in polarization.

Introduction

High power DC-DC converters such as modular multi-level converters or the bidirectional three phase dual active bridge (DAB3) [1] can be used to connect DC grids with different voltage levels [2]. Magnetic links, such as transformers, are an adequate choice to perform the step-up or step-down process between two different voltage levels [2]. The transformer winding voltage is directly proportional to the number of turns. Under fault condition, the transformer provides bidirectional galvanic isolation. Compared to conventional power transformers, which operate at 50 Hz or 60 Hz, medium frequency transformer result in a much smaller and compact component design. The transformer's iron losses must be examined at medium frequency to ensure a stable operating condition. This paper focuses on magnetic measurements of soft magnetic materials for medium frequency transformers. Modern material structures such as nanocrystalline materials and SiFe materials (silicon content up to 6.5%wt) are compared under sinusoidal conditions up to several kilohertz. Metrological characterization of the materials is done via an Epstein frame or a coil testing module. An advanced iron loss model, which is based on Bertotti's loss separation is used to describe the material behavior. The IEM-5-Parameter loss formula allows a comparison of hysteresis, eddy current, excess and nonlinear loss terms independently. The influence of different material properties is reflected in these parameters. In addition, the iron loss model is adapted to the nonsinusoidal excitation in a DAB3. High switching

frequencies and the influence of nonsinusoidal flux waveforms on the losses of ferromagnetic materials has been presented in [3–5]. However, all these proposed models to describe the core losses neglect to study each loss mechanism in a comparison of different ferromagnetic structured materials.

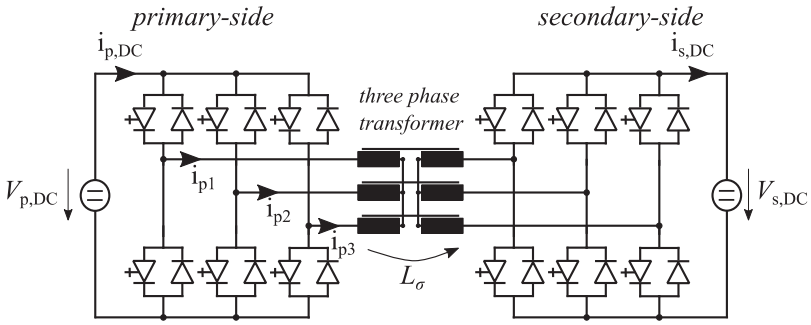

Fig. 1: Circuit diagram of a three-phase dual-active bridge converter (DAB3) [6].

A DAB3 has reduced switching losses, due to soft switching mode [7] and a high efficiency of the overall system is desired. Fig. 1 illustrates the transformer with its stray inductance L_σ in a schematic view of a three phase dual active bridge. The phase voltages and their corresponding flux densities per phase are shown in Fig. 2.

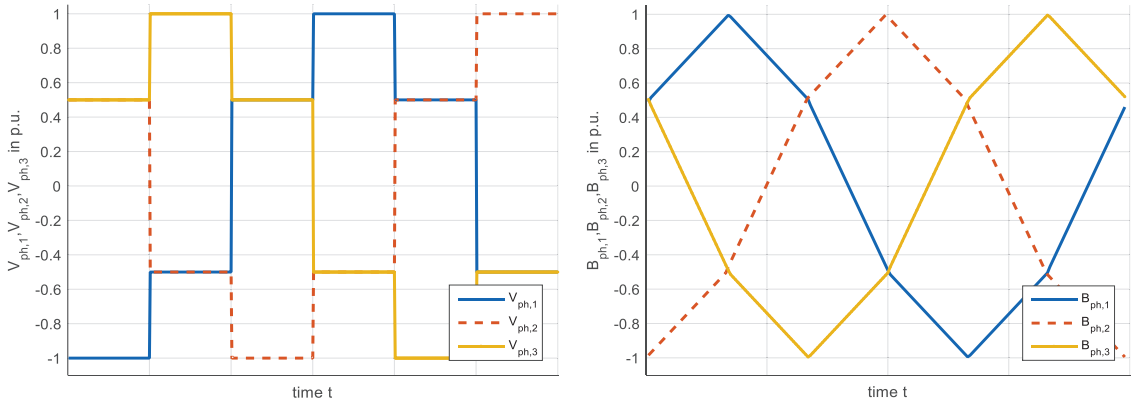

(a) (b)

Fig. 2: Idealized no-load voltage (a) and the resulting flux density per phase (b) for a DAB3 application [8].

Ferromagnetic materials for a medium frequency transformer

A ferromagnetic material should have low losses even at medium frequencies. The operating frequency range is set to f = 1 - 4 kHz to reduce volume, weight and costs. The iron losses of ferromagnetic materials depend on the flux density distribution and the frequency of the excitation. They also depend on other properties such as electric resistivity and the microstructures of the material such as grain size and grain orientation. Due to different compositions and manufacturing processes, the grain sizes, the electric resistivity and the thicknesses of the material varies. It has to be verified which combination of grain size, conductivity and material thickness result in minimized total core losses in case of medium frequency applications.

Nanocrystalline structure

The grain sizes of nanocrystalline materials are about 20 nm [9]. Compounds Fe, Si and B in combination with additives Nb and Cu and a modern process of manufacturing results in a material with a low saturation polarization. A reduced magnetostriction and a higher temperature resistance can be advantageous for a transformer design.

Standard SiFe

Conventional grain oriented silicon steels (SiFe) have grain sizes up to centimeters. The silicon content of the studied, high standard, grain oriented and non-oriented crystalline materials are increased up to 3.5%wt or 6.5%wt and the thickness is 0.35 mm or it is even lowered to 0.1 mm. This decreases the electric conductivity and as a result, the occurring eddy current losses are reduced. The silicon alloy also reduces the saturation polarization of the material. Due to the lower price of SiFe steel, it can be an alternative up to a particular frequency.

IEM-5-Parameter model

An iron loss separation model, which is based on Bertotti's loss equation [10] is used to describe the material behavior. The nonlinear material behavior for high values of flux densities is achieved by adding an additional term for saturation losses [11]. The iron loss model is developed to calculate the losses under sinusoidal excitations and allows to separate the losses into multiple loss components. The loss separation principle splits up the iron losses in hysteresis, classical eddy current, nonlinear and excess losses. The eddy current losses are represented by (3) and the parameter a_2 depends on thickness, density and electric resistivity as shown in (4). As derivated from Maxwell's equations, the parameter a_2 is an analytical value and decreases significantly for thin materials with a high electric resistivity.
All remaining material dependent parameters in (2) are determined by a mathematical fitting process, based on quasistatic and sinusoidal measurements. In case of grain oriented steel, the eddy current losses term is overestimated. For grain oriented steel, the parameter a_2 will not be calculated but also mathematically fitted to the measured loss values.
The terms with the parameters a_3 and a_4 consider an additional eddy current loss component due to nonlinear losses. The influence of excess losses is described by parameter a_5. The parameters allow a semi-physical interpretation of each loss term separately.

$$P_{\mathrm{IEM,5}} = P_{\mathrm{Hysteresis}} + P_{\mathrm{Eddycurrents}} + P_{\mathrm{nonlinear}} + P_{\mathrm{Excess}} \tag{1}$$

$$P_{IEM,5} = a_1 \cdot B^{\alpha} \cdot f + a_2 \cdot B^2 \cdot f^2 + a_2 \cdot a_3 \cdot B^{a_4+2} \cdot f^2 + a_5 \cdot B^{1.5} \cdot f^{1.5} \tag{2}$$

$$P_{\mathrm{Eddycurrents}} = a_2 \cdot B^2 \cdot f^2 \tag{3}$$

$$a_2 = \frac{\pi^2 \cdot d^2}{6 \cdot \rho \cdot \rho_{\mathrm{el}}} \tag{4}$$

Magnetic measurements

The measurements are performed with Epstein frames [12, 13] or a ring coil testing module [14]. The windings for the core specimens are applied manually. The mean magnetic path length l_{m} for the nanocrystalline toroidal core is listed in Table I.
All measurement instruments are limited to a maximum flux density of B = 2.0 T and a maximum frequency of f = 10 kHz.
The studied specimens are listed in Table I and the following measurements are performed:

- Quasistatic measurements, maximum change rate: $\frac{\mathrm{d}B}{\mathrm{d}t} = 30$ mT/s
- Sinusoidal polarization
- DAB3 polarization (Fig. 2)

Table I: Overview of the considered ferromagnetic specimens.

material		type of specimen	thickness in mm	electric resistivity in $\mu\Omega$m
JFE JNEX900	SiFe (NO)	Epstein	0.10	0.82
NO10	SiFe (NO)	Epstein	0.10	0.52
H80-23L	SiFe (GO) - RD	Epstein	0.23	0.48
H85-27L	SiFe (GO) - RD	Epstein	0.27	0.48
M150-30S	SiFe (GO) - RD - ANN	Epstein	0.30	0.48
Vitroperm 500F	Nanocrystalline	Core, l_m = 178mm	0.02	1.20

(RD = rolling direction. ANN = annealed. NO = non-oriented. GO = grain-oriented.)

Results of sinusoidal excitation

The specific core losses of the proposed materials are shown in Fig. 3 for f = 1 kHz. The thickness of the materials is directly correlated to the specific losses. Most of the SiFe materials perform similar at f = 1 kHz, especially at low flux densities. Only the material JNEX900 benefits from the combination of only 0.1 mm thickness of and a silicon content of 6.5%wt. This material produces at B = 0.8 T about 12.6 W/kg iron losses. The materials H80-23L, which is a grain oriented steel, produces about 23.4 W/kg at B = 0.8 T which is an increase of almost factor of two.

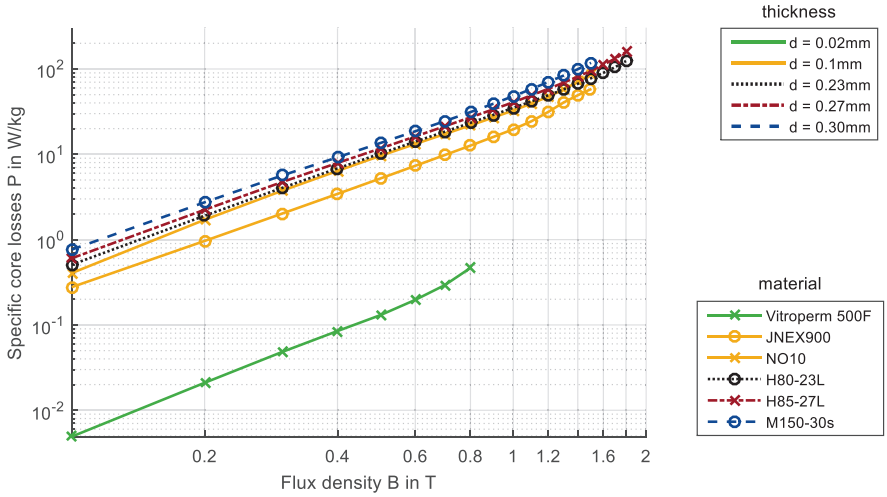

Fig. 3: Sinusoidal excitation. Frequency f = 1 kHz.

The results of the sinusoidal measurements for f = 4 kHz are shown in Fig. 4, the high silicon content in combination with d = 0.1 mm thickness performs best of all SiFe again. This is also expected for higher frequencies and mainly resulting from reduced eddy current and excess losses at high frequencies. The measured specific core losses increase strongly for higher flux density values.
The non-grain-oriented material NO10 has a thickness of d = 0.1 mm but a low specific resistivity. This results in a material behavior which is competitive to a thicker material like H80-23L or H85-27L at f = 1 kHz. At f = 4 kHz the thinner, non-grain-oriented material benefits from reduced eddy current losses compared to a thicker grain-oriented material (Fig. 3 and Fig. 4).

 ISBN: 9789075815252 and CFP16850-USB

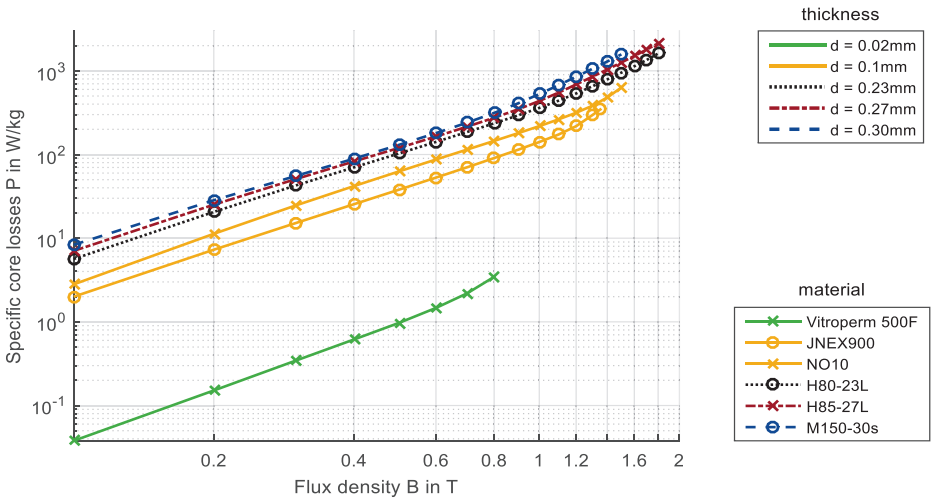

Fig. 4: Sinusoidal excitation. Frequency $f = 4$ kHz.

All measurements with the nanocrystalline material showed a significant lower loss generation compared to standard materials. But, compared to standard SiFe materials, the measured saturation flux density is low. A detailed extraction of the datapoints for $f = 1$ kHz and $f = 4$ kHz is given in Table II.

Table II: Measured specific core losses.

frequency	material	Specific core losses $P(B)$ in W/kg			
		$B = 0.1$ T	$B = 0.2$ T	$B = 0.5$ T	$B = 0.8$ T
$f = 1$ kHz	Vitroperm 500F	0.01	0.02	0.13	0.47
	JNEX900	0.28	0.96	5.21	12.65
	NO10	0.41	1.71	9.59	21.84
	H80-23L	0.51	1.90	10.20	23.40
$f = 4$ kHz	Vitroperm 500F	0.04	0.15	0.97	3.45
	JNEX900	2.00	7.28	38.00	90.73
	NO10	2.81	11.28	62.90	145.40
	H80-23L	5.64	20.61	103.10	235.80

Consideration of the transformer's cooling system

Usually medium frequency transformer are cooled by a forced cooling system. To consider a cooling system, the maximum dissipation losses have to be limited. The maximum loss generation is dependent on various design parameter such as surface area, heat transfer coefficient and copper losses. Table III summarizes maximum allowed flux density values for an example of 10W/kg core losses. The value is chosen based on [15] and [16].

Table III: Maximum flux densities considering an allowed loss dissipation.

material	B_{max} (P=10W/kg), $f = 1$ kHz	B_{max} (P=10W/kg), $f = 4$ kHz
JFE JNEX900	0.71 T	0.23 T
NO10	0.47 T	0.17 T
H80-23L	0.49 T	0.13 T
H85-27L	0.45 T	0.12 T
M150-30S	0.41 T	0.11 T

All listed materials with their respective allowed flux densities in combination with the listed frequency dissipates the same amount of losses under sinusoidal excitations. The amount of required material is directly influenced by the maximum allowed flux density and reflected in costs, weight and volume of the magnetic core. Any deviation due to different cooling surface sizes are neglected. In case of silicon

iron materials, the allowed flux density of material M150-30S is only 57% compared to JNEX900. In case of f = 4 kHz, the allowed flux density is in fact less than half.
A detailed frequency dependency of the nanocrystalline material is shown in Fig. 5. Under the perspective of equal heat generation, even at saturation the nanocrystalline material produces less losses at f = 1 kHz or f = 4 kHz. Compared with JNEX900 in Table III, to generate the same losses of P = 10 W/kg at B = 0.71 T, the frequency can be increased up to f = 9 kHz in case of the nanocrystalline material.

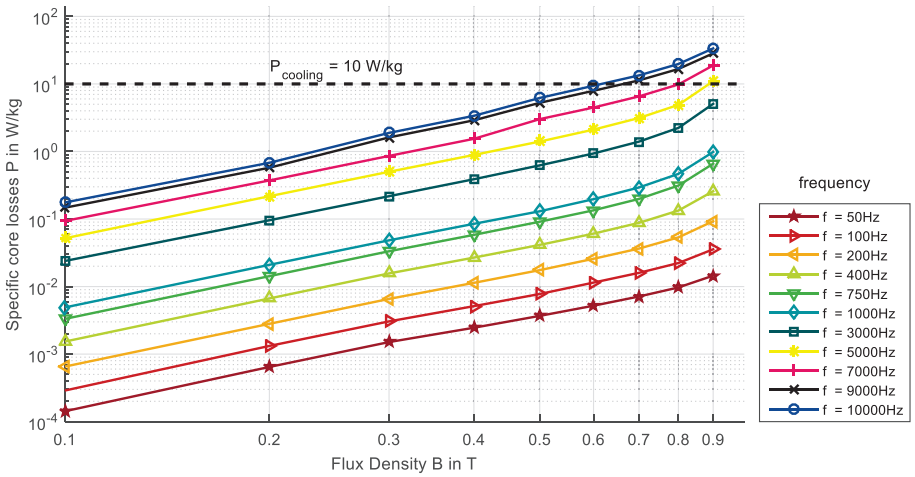

Fig. 5: Sinusoidal excitation. Measured iron losses up to f = 10 kHz. Material: Vitroperm 500F.

Material parameters

To clarify the influence of each loss mechanism in the studied frequency and flux density range, the loss terms are shown separated Fig. 6. Hysteresis, eddy current and excess losses are the dominating loss phenomena in this flux density range. The influence of the nonlinear loss term can be neglected in the studied flux density range below B = 0.9 T. The remaining parameters for the studies materials are listed in Table IV.

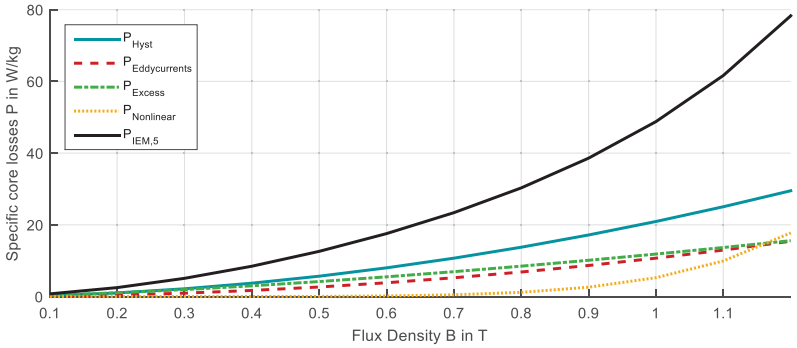

Fig. 6: Example of loss separation model. Material: JFE 10JNEX900. f = 2 kHz. Sinusoidal excitation.

With the given parameters in Table IV the influence of the loss terms can be computed at the given frequency and flux density combinations as listed in Table III.
As shown in Table IV, the eddy current parameter a_2 is directly correlated to the thickness and resistivity of the material. At even higher frequencies, the eddy current loss term dominate the losses due to a quadratic influence of flux density and frequency.

Table IV: Hysteresis, eddy current and excess loss parameters.

material	parameter a_1 $\cdot 10^{-3}$	parameter α	parameter a_2 $\cdot 10^{-6}$	parameter a_5 $\cdot 10^{-3}$
JFE 10JNEX900	10.47	1.880	2.678	0.133
NO10	20.91	1.781	4.135	0.179
H80-23L	1.404	1.511	4.875	0.703
H85-27L	2.830	1.998	5.558	0.734
M150-30S	2.645	1.514	6.240	0.719
Vitroperm 500F	0.575	2.090	0.072	0.013

It is assumed, that the excess losses can be neglected in case Vitroperm 500F. The influence of parameter a_5 when compared to other materials is low. The nanocrystalline structure does not exist of large domain walls and as a result, the movement of magnetic domain walls due to local changes in magnetic directions is hardly present.

Discussion of DAB3 excitation

To clarify the influence of the nonsinusoidal excitation (Fig. 2) in DAB3 application, a comparison between the iron losses of sinusoidal and DAB3 excitation is made with JNEX900. The hysteresis loop at two different frequencies is shown in Fig. 7. The area spanned by the hysteresis loop is in case of DAB3 conditions smaller. This area is directly proportional to the needed energy per magnetization cycle.

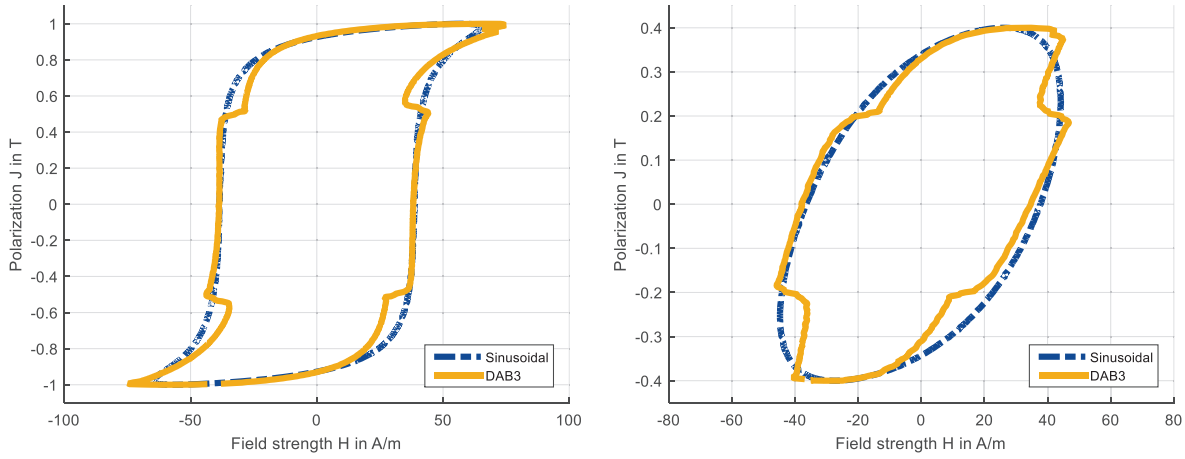

Fig. 7: Hysteresis loops. Material: JFE 10JNEX900. Frequency $f = 1$ kHz and polarization $J = 1.0$ T (a). Frequency $f = 4$ kHz and polarization $J = 0.4$ T (b).

Comparison of losses between sinusoidal and DAB3 excitation

Fig. 8 shows that the specific iron losses for DAB3 excitation tend to be smaller. The material in this study is JFE JNEX900. The relative deviation compared to sinusoidal excitation is given in Table V. In case of DAB3 excitation, the iron losses turn out to be up to 10% smaller. The desired form factor of DAB3 excitation, which indicated the goodness of a measurement, is at even higher values of flux density unachievable.

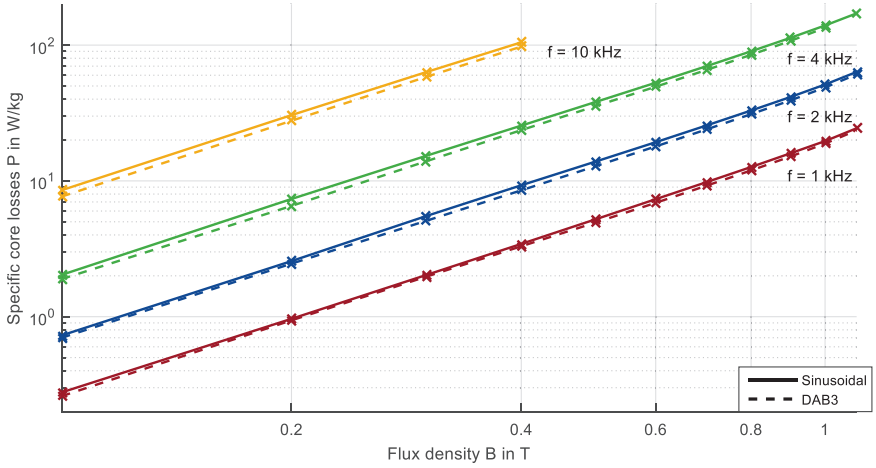

Fig. 8: Solid lines represents sinusoidal excitation and dashed lines represent DAB3 excitation. Material: JNEX 900.

It is assumed, that the noticed, small deviation in reduced losses is also valid for other materials.

Table V: Relative reduced iron losses in case of DAB3 compared to sinusoidal.

flux density $\widehat{B}$ in T	Relative deviation $\frac{\lvert P_{\mathrm{DAB3}} - P_{\mathrm{SIN}} \rvert}{P_{\mathrm{SIN}}}$			
	$f = 1$ kHz	$f = 2$ kHz	$f = 4$ kHz	$f = 10$ kHz
0.1	6.2 %	3.9 %	6.9 %	10.2 %
0.2	2.6 %	4.3 %	11.1 %	9.2 %
0.5	5.3 %	7.6 %	6.7 %	/
0.8	5.5 %	6.0 %	5.7 %	/
1.0	4.1 %	4.9 %	3.9 %	/

Adapted harmonic loss separation model

In a dual active bridge application the polarization signal differs from a sinusoidal polarization signal (Fig. 2). A comparison of the signals with the same amplitude can be seen in Fig. 9 (a). A fast Fourier transform (FFT) of the DAB3 polarization is shown in Fig. 9 (b). Each harmonic component has an influence on the occurring iron losses. The high frequency harmonics and their corresponding amplitude need to be considered in an iron loss calculation.

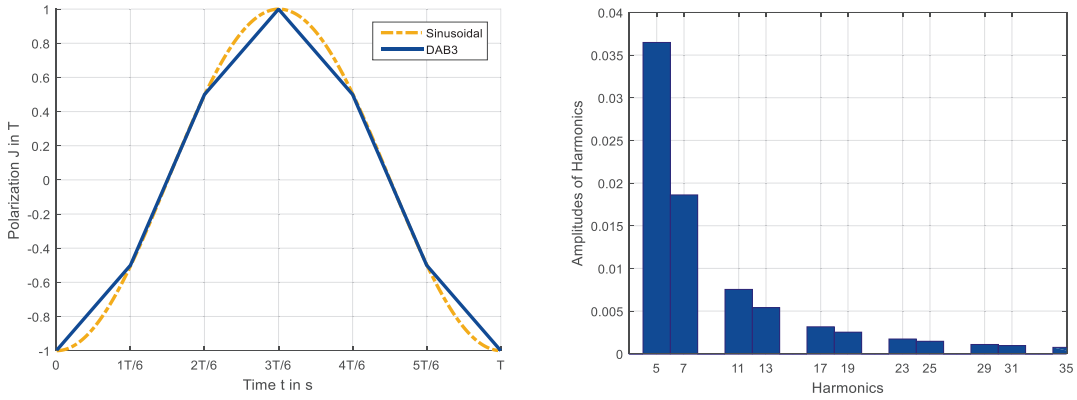

(a) (b)

Fig. 9: Comparison between DAB3 and sinusoidal excitation and harmonics in case of DAB3 excitation (from left to right). The amplitude of the first harmonic (fundamental wave) is $J = 0.92$ T.

The high frequency harmonics can be considered by introducing an accumulation of all frequency components f_i and flux density components B_i. The accumulation is included in the eddy current and excess losses terms. The material parameters are obtained from the sinusoidal model:

$$P_{\mathrm{IEM,5,harmonics}} = a_1 \cdot B_1^{\alpha} \cdot f_1 + \sum_i^{\infty} (a_2 \cdot B_i^2 \cdot f_i^2) + a_2 \cdot a_3 \cdot B_1^{a_4+2} \cdot f_1^2 + \sum_i^{\infty} (a_5 \cdot B_i^{1.5} \cdot f_i^{1.5}) \quad (5)$$

A comparison between the adapted, harmonic loss model (5) and the measured losses is shown in Fig. 10. The modified loss model results are in a good agreement with the measured values. The harmonics cannot be neglected.

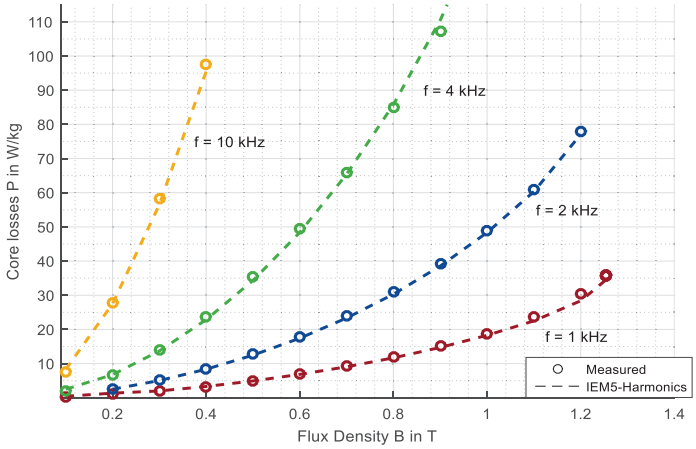

Fig. 10: Measured losses under presence of DAB3 excitation compared with calculated losses. Material: 10JNEX900.

Conclusions

In this paper different ferromagnetic materials are studied for medium frequency applications such as transformers. Magnetic measurements of standard SiFe and nanocrystalline materials are performed by using a standardized measurement instrument. The influences of frequencies up to several kilohertz are studied by using the IEM-5-Parameter formula, a semi-physical iron loss separation model. The different loss terms are evaluated parameters in a feasible range of flux density and frequency and the parameters of the materials are listed. These parameters represent material properties, which allow a direct comparison. It is shown, that for frequencies up to $f = 1$ kHz, grain oriented materials with a thickness of $d = 0.23$ mm are competitive with thinner materials like NO10. But at $f = 4$ kHz, the grain orientation is not advantageous compared to non-oriented materials with $d = 0.1$mm. The thickness or the electric resistivity of the material is more important at high frequency applications due to reduced eddy current influences. This behavior is reflected in the eddy current and excess-loss parameters a_2 and a_5. The iron losses in case of Vitroperm 500F are much lower compared to all other materials in this study. For the same amount of iron losses, the frequency of the excitation signal could be increased by a factor nine up to $f = 9$ kHz compared to JNEX900. But, the saturation flux density of the nanocrystalline material is low compared to standard SiFe. It is shown, that the influence of the excess losses are strongly reduced in case of nanocrystalline materials. The nanocrystalline structure does not consist of large grains or domain walls where the additional eddy currents occur.

The excitation and voltage signal in the case of a dual active bridge application are presented. The iron losses under DAB3 excitation tend to be about 5-10% smaller compared to the sinusoidal measurements. The hysteresis loop of the measurements are shown and the reduced losses are reflected in the spanned area. The harmonics in the DAB3 excitation signal are obtained by using a fast Fourier transform. The IEM-5-Parameter formula is adapted to these harmonics. A good agreement between calculated and measured DAB3 losses is shown.

For medium frequency application, the ferromagnetic material selection plays an important key role in case of thermal balance and efficiency. Modern materials such as nanocrystalline can help to reduce the generated iron losses.

References

[1] Engel S. , Stieneker M. , Soltau N. , Rabiee S. , Stagge H. and De Doncker R. W.: Comparison of the Modular Multilevel DC Converter and the Dual-Active Bridge Converter for Power Conversion in HVDC and MVDC Grids, Power Electronics, IEEE Transactions on, vol. 30, no. 1, pp. 124–137, 2015.

[2] Islam M. , Guo Y. and Zhu J, Power Converters for Medium Voltage Networks. Berlin, Heidelberg: Springer Berlin Heidelberg, 2014.

[3] Reinert J. , Brockmeyer A. and De Doncker R. W.: Calculation of losses in ferro- and ferrimagnetic materials based on the modified Steinmetz equation, Industry Applications, IEEE Transactions on, vol. 37, no. 4, pp. 1055–1061, 2001.

[4] Soltau N. , Eggers D. , Hameyer K. and De Doncker R. W.: Iron Losses in a Medium-Frequency Transformer Operated in a High-Power DC–DC Converter, IEEE Transactions on Magnetics, vol. 50, no. 2, pp. 953–956, 2014.

[5] Mayuri R. , Sinnou N. and Ilango K.: Eddy current loss modelling in transformer iron losses operated by PWM inverter, Joint International Conference on Power Electronics, Drives and Energy Systems (PEDES) & Power India, 2010.

[6] Engel S. , Soltau N. , Stagge H. and De Doncker R. W.: Dynamic and Balanced Control of Three-Phase High-Power Dual-Active Bridge DC–DC Converters in DC-Grid Applications, Power Electronics, IEEE Transactions on, vol. 28, no. 4, pp. 1880–1889, 2013.

[7] Hoang K. and Wang J.: Design optimization of high frequency transformer for dual active bridge DC-DC converter, International Conference on Electrical Machines (ICEM), 2012.

[8] Lenke R.: A contribution to the design of isolated DC-DC converters for utility applications, vol. 6, 2012.

[9] Herzer G.: Modern soft magnets: Amorphous and nanocrystalline materials, The Diamond Jubilee Issue Materials Challenges in Tomorrow's World Selected Topics in Materials Science and Engineering, vol. 61, no. 3, pp. 718–734, 2013.

[10] Bertotti G.: General properties of power losses in soft ferromagnetic materials, Magnetics, IEEE Transactions on, vol. 24, no. 1, pp. 621–630, 1988.

[11] Eggers D. , Steentjes S. and Hameyer K.: Advanced Iron-Loss Estimation for Nonlinear Material Behavior, IEEE Transactions on Magnetics, vol. 48, no. 11, pp. 3021–3024, 2012.

[12] Magnetic materials: Matériaux magnétiques, 3rd ed. Geneva: International Electrotechnical Commission, 2008.

[13] DIN EN 60404-2, Magnetische Werkstoffe – Teil 2: Verfahren zur Bestimmung der magnetischen Eigenschaften von Elektroband und -blech mit Hilfe eines Epsteinrahmens.

[14] DIN EN 60404-6, Magnetische Werkstoffe – Teil 6: Verfahren zur Messung der magnetischen Eigenschaftenweichmagnetischer und pulverförmiger Werkstoffe bei Frequenzen im Bereich 20 Hz bis 200 kHz mit Hilfe von Ringproben (IEC 60404-6:2003).

[15] Villar I. , Garcia-Bediaga A. , Viscarret U. , Etxeberria-Otadui I. and Rufer A.: Proposal and validation of medium-frequency power transformer design methodology, 2011.

[16] Villar I. , Mir L. , Etxeberria-Otadui I. , Colmenero J. , Agirre X. and Nieva T.: Optimal design and experimental validation of a Medium-Frequency 400kVA power transformer for railway traction applications, 2012.